

Dielectric Relaxation of NaClO_4 Solutions in Formamide, N-Methylformamide, and N,N-Dimethylformamide

J. Barthel, K. Bachhuber, and R. Buchner

Institut für Physikalische und Theoretische Chemie, Universität Regensburg, D-93040 Regensburg

Z. Naturforsch. **50a**, 65–74 (1995); received October 22, 1994

Dedicated to Prof. Hitoshi Ohtaki on the occasion of his 60th birthday

Complex permittivity spectra in the frequency range $0.95 \leq \nu/\text{GHz} \leq 89$ for N,N-dimethylformamide (DMF), N-methylformamide (NMF), formamide (FA) and their solutions of NaClO_4 are investigated to study the change of liquid structure and dynamics arising from the availability of one hydrogen-bond acceptor site together with no (DMF), one (NMF), or two (FA) donor sites on the same molecule. Three solvent relaxation processes are observed for NMF and two for FA and DMF. The relaxation parameters are used to determine solvation numbers. They show that ion-solvent interactions lead to a reduction of the average length of the H-bonded NMF chains but have only moderate influence on the FA structure. An additional solute relaxation process in DMF solutions is due to the diffusion-controlled formation and decomposition of solvent-shared ion pairs.

Key words: Dielectric relaxation, Formamides, Solvation, Solvent dynamics, Ion association.

1. Introduction

Due to high polarity and strong solvating power combined with a large liquid state range, formamide (FA) as well as its derivatives N-methylformamide (NMF) and N,N-dimethylformamide (DMF) are interesting solvents in research and technical processes [1, 2, 3]. In addition, NMF is the simplest molecule incorporating the biologically important $\text{O}=\text{C}-\text{NHR}$ configuration characteristic for peptides. Therefore the solution properties of the amides have extensively been studied, see [4, 5]. Diffraction experiments [6, 7, 8, 9, 10] reveal the impact of hydrogen bonding on the structure of the neat liquids ranging from the random distribution of molecular dipole orientations in DMF via the formation of flexible chains with preferred parallel orientation of the molecular moments μ_i in NMF to the three-dimensional arrangement of FA molecules, where the formation of ring-dimers reduces the macroscopic dipole moment $M = \sum \mu_i$ compared to NMF.

Much less is known about the dynamics of the amides, especially the cooperative processes arising from hydrogen bonding, and on the structural implications of ion solvation. Such processes can be successfully investigated by dielectric relaxation studies [11, 12] provided the complex permittivity spectra

$\hat{\epsilon}(\omega) = \epsilon'(\omega) - i\epsilon''(\omega)$, $\omega = 2\pi\nu$, are recorded with high accuracy over a wide range of frequencies ν , a requirement only incompletely met by the older dielectric studies of electrolyte solutions in the formamides [13, 14, 15]. The frequency dependence of the complex permittivity, $\hat{\epsilon}(\omega)$, probes the individual contributions to the relaxation of the sample polarization $P(t)$ after a change of the applied electrical field provided their relaxation times τ_i are sufficiently different. In electrolyte solutions these processes may arise from the reorientation of individual solvent dipoles, from the kinetics of ion-pair formation, and from structural relaxation of the H-bonded aggregates. Fast intramolecular contributions due to molecular polarizability are outside the observation window of interest and are subsumed in the “infinite frequency” permittivity ϵ_∞ .

In this contribution we present results from complex permittivity measurements in the frequency range $0.95 \leq \nu/\text{GHz} \leq 89$ for solutions of NaClO_4 in FA, NMF, and DMF at 25°C , supplementing the preliminary report on the dielectric properties of the neat solvents [16].

2. Experimental

2.1. Materials

The solvents formamide (Merck *p.A.*), N-methylformamide (Fluka *purum*), and N,N-dimethylform-

Reprint requests to Prof. J. Barthel.

0932-0784 / 95 / 0100-0065 \$ 06.00 © – Verlag der Zeitschrift für Naturforschung, D-72027 Tübingen



Dieses Werk wurde im Jahr 2013 vom Verlag Zeitschrift für Naturforschung in Zusammenarbeit mit der Max-Planck-Gesellschaft zur Förderung der Wissenschaften e.V. digitalisiert und unter folgender Lizenz veröffentlicht: Creative Commons Namensnennung-Keine Bearbeitung 3.0 Deutschland Lizenz.

Zum 01.01.2015 ist eine Anpassung der Lizenzbedingungen (Entfall der Creative Commons Lizenzbedingung „Keine Bearbeitung“) beabsichtigt, um eine Nachnutzung auch im Rahmen zukünftiger wissenschaftlicher Nutzungsformen zu ermöglichen.

This work has been digitalized and published in 2013 by Verlag Zeitschrift für Naturforschung in cooperation with the Max Planck Society for the Advancement of Science under a Creative Commons Attribution-NoDerivs 3.0 Germany License.

On 01.01.2015 it is planned to change the License Conditions (the removal of the Creative Commons License condition “no derivative works”). This is to allow reuse in the area of future scientific usage.

amide (Fluka *p.A.*) were dried over molecular sieve (FA: Merck 0.3 nm; DMF, NMF: Merck 0.4 nm) for at least 7 days and then fractionally distilled under reduced pressure (≈ 2 Torr) using a closed apparatus with two packed columns in line [17]. Gaschromatographically determined organic impurities amounted to less than 0.08% for all batches used in the experiments, residual water in FA < 130 ppm, in NMF < 150 ppm, and in DMF < 100 ppm. Column 3 of Table 1 reports the maximum conductivity of the purified solvents. To monitor eventual solvent decomposition during the measurements, the data refer to purity checks performed after all experiments, i.e. 4–5 weeks after distillation.

NaClO₄ (Merck *p.A.*) was recrystallized twice from water and vacuumdried at 140 °C over Sicapent® (Merck) for 7 days. Sample preparation by weight and experiments were carried out under an atmosphere of dry nitrogen.

2.2. Measurements

Complex permittivities of the solutions at 25.00 \pm 0.01 °C were determined at 28 to 31 frequencies with the help of one coaxial (0.95 to 2.5 GHz) and five waveguide devices (4 to 89 GHz) using the method of travelling waves. Details of the equipment are given in [18, 19]. The determined wavelengths $\lambda_M(\nu)$ and attenuation coefficients $\alpha(\nu)$ directly yield the complex generalized permittivity

$$\hat{\eta}(\omega) = \hat{\varepsilon}(\omega) - i \frac{\hat{\kappa}(\omega)}{\omega \varepsilon_0} \quad (1)$$

comprising dielectric displacement and ohmic contribution of the sample response; ε_0 is the permittivity of the vacuum. At $\nu < 40$ GHz a precision of 1.5% for the real part of $\hat{\eta}(\omega)$ and of 2.5% for the imaginary part is achieved; at higher frequencies we have 3% for η' and η'' .

To obtain the complex permittivity $\hat{\varepsilon}(\omega)$ from (1), the common assumption is made that $\hat{\kappa}$ equals the real part $\kappa(0) = \kappa$ obtained at quasi-static frequencies ($\nu \rightarrow 0$). These conductivity data were determined with a precision of 0.1% using standard methods of our laboratory [17]. Densities ρ for the conversion of solute molalities to molar concentrations c were obtained with a vibrating-tube density meter (Paar DMA60/DMA602) using air and degassed water as the references. Viscosities η were determined with the help of an Ubbelohde viscometer with optoelectronic

Table 1. Density ρ , conductance κ , and viscosity η of NaClO₄ solutions of concentration c in FA, NMF, and DMF at 25 °C.

	c mol dm ⁻³	ρ kg m ⁻³	κ $\Omega^{-1} \text{ m}^{-1}$	η 10 ⁻³ Pa s
FA	0.0	1129.1	0.0081	3.29
	0.14256	1138.6	0.3110	3.49
	0.29613	1148.7	0.5760	4.08
	0.52637	1163.9	0.9010	4.82
	0.9109	1189.0	1.2794	6.36
NMF	0.0	998.4	0.0006	1.73
	0.10059	1005.9	0.3818	1.82
	0.24444	1017.0	0.7922	1.97
	0.49791	1036.3	1.3676	2.28
	0.89030	1066.2	1.8471	2.88
DMF	0.0	943.83	0.00002	0.802
	0.07183	950.21	0.41691	0.858
	0.12912	955.26	0.68615	0.894
	0.49378	986.97	1.8515	1.20
	1.0200	1031.8	2.4735	1.90

detection (Schott AVS/G) using water as the reference. The results for ρ , κ and η are summarized in Table I.

3. Results and Discussion

3.1. Relaxation Models

The formal description of the complex permittivity spectra was achieved by fitting a semi-empirical relaxation model expressed as the sum of Havriliak-Negami type processes

$$\hat{\varepsilon}(\omega) = \varepsilon_\infty + (\varepsilon - \varepsilon_\infty) \sum_{j=1}^n \frac{g_j}{[1 + (i\omega)^{1-\alpha_j}\beta_j]} \quad (2)$$

comprising n discernable relaxation processes j of relaxation time τ_j and weight g_j

$$g_j = \frac{\varepsilon_j - \varepsilon_{j\infty}}{\varepsilon - \varepsilon_\infty}; \quad \varepsilon_1 = \varepsilon; \quad \varepsilon_{j\infty} = \varepsilon_{j+1}; \quad \varepsilon_{n\infty} = \varepsilon_\infty$$

with the special cases $\alpha_j = 0$, $0 < \beta_j < 1$ (Davidson-Cole process), $0 < \alpha_j < 1$, $\beta_j = 1$ (Cole-Cole process), and $\alpha_j = 0$, $\beta_j = 1$ (Debye process). $\varepsilon = \varepsilon'(0)$ is the static permittivity of the solution. Figure 1 shows a typical example for the investigated solutions and defines the more informative notation subsequently used in the text, where the index s designates that the parameter originates from a relaxation process of the *solvent* and IP represents the *solute*.

When only data up to 89 GHz are considered, the normalized sum of squared residuals, χ^2 , does not allow to discriminate between several possible models for the neat solvents [16]. Inclusion of far-infrared

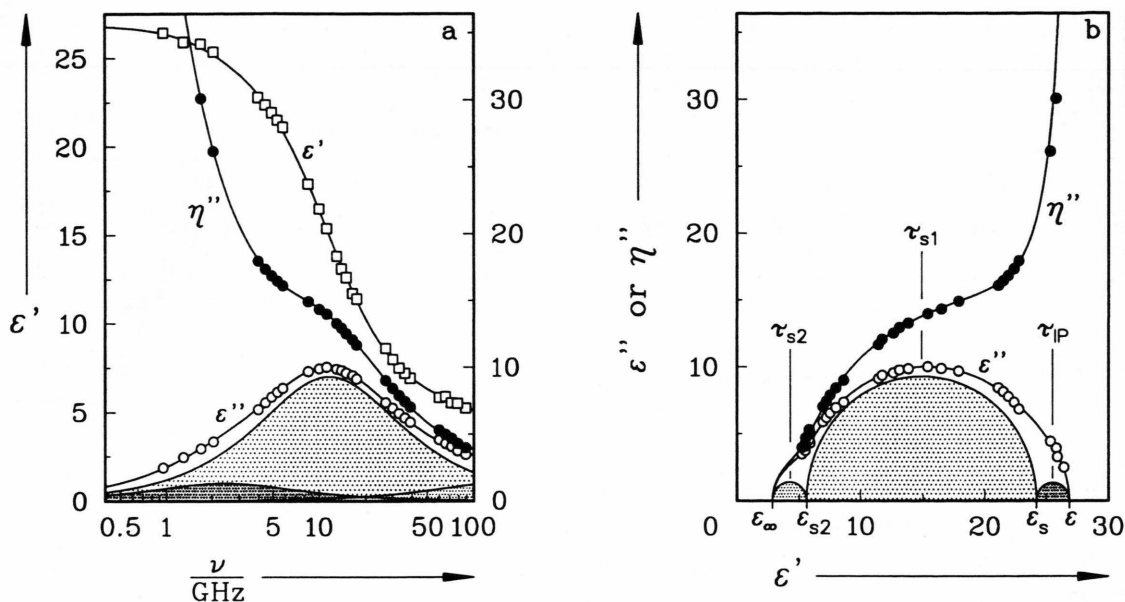


Fig. 1. Complex permittivity spectrum of a 1.02 mol dm⁻³ solution of NaClO₄ in DMF at 25°C. a) Frequency dependence of dielectric dispersion and loss, $\epsilon'(\nu)$ resp. $\epsilon''(\nu)$, and of the total loss $\eta''(\nu) = \epsilon'' + \kappa/(\omega \epsilon_0)$; b) the corresponding Argand diagrams. The shaded areas represent the individual contributions of the ion-pair (IP) and of the solvent relaxation processes s1 and s2.

(FIR) data in the range $234 \leq \nu/\text{GHz} \leq 293$ for DMF [20] and $146 \leq \nu/\text{GHz} < 293$ for NMF [21] yields an unambiguous decision. The relaxation of DMF is governed by two Debye processes of parameters $\epsilon_s = 37.25$, $\tau_{s1} = 10.36$ ps, $\epsilon_{s2} = 4.41$, $\tau_{s2} = 0.74$ ps, $\epsilon_\infty = 2.84$. The slightly different set of parameters compared to [16] results from a re-determination of $\hat{\epsilon}(\omega)$ in the 13 to 17.5 GHz region with improved cell design and from more precise far-infrared data compared to [22]. For NMF three Debye processes are found with parameters $\epsilon_s = 183.3$, $\tau_{s1} = 127.6$ ps, $\epsilon_{s2} = 6.13$, $\tau_{s2} = 7.9$ ps, $\epsilon_{s3} = 4.60$, $\tau_{s3} = 0.79$ ps, $\epsilon_\infty = 3.20$.

It might be argued that fitting a Debye process of $\tau \approx 0.8$ ps to complex permittivity spectra of asymmetric rotors with large moments of inertia is questionable. Indeed, the experimental FIR spectrum of DMF exhibits a considerable half width of the libration band centered around 70 cm^{-1} (2000 GHz) which distinctly exceeds the result obtained from the Gaussian-cage model [20], and NMF exhibits a strong absorption ($\alpha_{\text{max}} = 695 \text{ Np cm}^{-1}$ at 116 cm^{-1}) with a large low-frequency tail [21]. However, for the electrolyte solutions only the assumption of two Debye

processes for the solvent relaxation of DMF and of three processes for NMF yields consistent results with a minimum scatter of the obtained relaxation parameters as functions of electrolyte concentration c , and allows the interpretation of the results in terms of physical processes. This argument also allows to select the combination of a slow Cole-Cole and a fast Debye process as most appropriate for FA and its NaClO₄ solutions (parameters at $c = 0$: $\epsilon_s = 108.8$, $\tau_{s1} = 37.32$ ps, $\alpha_{s1} = 0.006$, $\epsilon_{s2} = 7.08$, $\tau_{s2} = 1.2$ ps, $\epsilon_\infty = 4.48$). An additional low-frequency Debye dispersion, parameters ϵ , τ_{IP} , $\epsilon_{IP\infty} = \epsilon_s$, arises at increasing electrolyte concentrations for DMF solutions due to ion-pair (IP) formation. Tables 2–4 summarize the results and the corresponding χ^2 . To reduce the number of adjustable parameters for the electrolyte solutions covering $\nu \leq 89 \text{ GHz}$ the permittivities ϵ_∞ were fixed to the corresponding values of the neat solvents for NMF (Table 3) and DMF (Table 4). The error margins given in Tables 2–4 are the maximum deviations from appropriate polynomial fits to the ϵ_j and τ_j vs. c . These quantities yield a more reasonable estimate of the precision than the relative uncertainties of the parameters from non-linear least squares routines.

Table 2. Relaxation parameters of NaClO₄ solutions in formamide at 25 °C.

c mol dm ⁻³	$\varepsilon = \varepsilon_s$	τ_{s1} ps	α_{s1}	ε_{s2}	τ_{s2} ps	ε_∞	χ^2
	± 0.5	± 0.04	± 0.004	± 0.15	± 0.3	± 0.4	
0.0	108.8	37.32	0.006	7.08	1.2	4.5	0.06
0.14256	105.2	37.48	0.014	6.92	1.1	4.9	0.15
0.29613	100.8	37.60	0.012	7.27	1.6	5.2	0.08
0.52637	94.9	37.89	0.018	7.34	1.3	4.7	0.08
0.9109	86.7	38.66	0.023	7.77	1.8	5.3	0.14

Table 3. Relaxation parameters of NaClO₄ solutions in N-methylformamide at 25 °C.

c mol dm ⁻³	$\varepsilon = \varepsilon_s$	τ_{s1} ps	ε_{s2}	τ_{s2} ps	ε_{s3}	τ_{s3} ps	ε_∞	χ^2
	± 0.6	± 0.8	± 0.08	± 0.3	± 0.07	± 0.1		
0.0	183.3	127.6	6.13	7.9	4.60	0.79	3.20	0.36
0.10059	169.2	123.9	6.32	7.8	4.56	0.8	3.20 ^F	0.34
0.24444	148.7	116.5	6.51	8.2	4.73	0.9	3.20 ^F	0.21
0.49791	121.5	107.8	7.14	9.5	4.88	0.8	3.20 ^F	0.21
0.89030	93.3	99.4	7.86	10.5	5.08	0.8	3.20 ^F	0.18

^F parameter not adjusted.Table 4. Relaxation parameters of NaClO₄ solutions in N,N-dimethylformamide at 25 °C.

c mol dm ⁻³	ε	τ_{IP} ps	ε_s	τ_{s1} ps	ε_{s2}	τ_{s2} ps	ε_∞	χ^2
	± 0.2	± 10	± 0.15	± 0.03	± 0.07	± 0.1		
0.0	—	—	37.25	10.36	4.41	0.74	2.84	0.004
0.07183	36.8	155	35.76	10.49	4.62	0.8	2.84 ^F	0.019
0.12912	36.3	167	34.91	10.64	4.65	0.9	2.84 ^F	0.017
0.49378	31.8	103	29.82	11.57	4.97	0.9	2.84 ^F	0.009
1.0200	26.9	67	24.19	13.70	5.63	1.0	2.84 ^F	0.009

^F parameter not adjusted.

3.2. Solvent Permittivity and Solvation

The static permittivity of the solvent in the solutions, ε_s , is a sensitive probe for the impact of ion-solvent interactions on the liquid structure. The three amide systems of this study exhibit the typical non-linear decrease of ε_s with electrolyte concentration

$$\Delta\varepsilon_s(c) = \varepsilon_s(c) - \varepsilon_s(0) = -\delta_\varepsilon c + \beta_\varepsilon c^2 \quad (3)$$

with the parameters δ_ε and β_ε summarized in Table 5. Figure 2 shows the relative change $\Delta\varepsilon_s(c)/\varepsilon_s(0)$ as a function of the molar ratio c/c_s of electrolyte to solvent

in the solution, allowing a direct comparison of the influence of NaClO₄ on the permittivity of the formamides.

The breakdown of the NMF permittivity to about 50% of $\varepsilon_s(0)$ at a molar ratio of 5:100 shows that the structure of NMF is strongly affected by ion-solvent interactions. This behaviour is similar to methanol solutions [23, 24] and suggests that the average length of the hydrogen-bonded chains of solvent molecules is reduced. The static permittivity of DMF is much less affected, and at least at low concentrations the behaviour is comparable to NaClO₄ solutions of

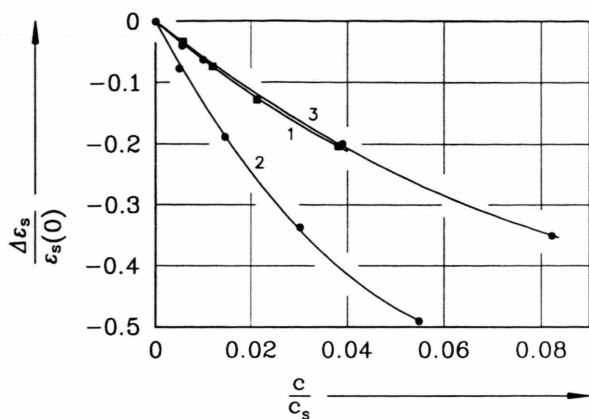


Fig. 2. Relative change $\Delta\epsilon_s/\epsilon_s(0)$ of the solvent permittivity, $\epsilon_s(c)$, as a function of the molar ratio c/c_s of NaClO₄ to solvent in the solution at 25°C for 1: FA, 2: NMF, and 3: DMF.

Table 5. Parameters δ_ϵ and β_ϵ of (3) and solvation numbers Z_{IB} according to (4) without ($\xi = 0$) and with correction for kinetic depolarization under *stick* or *slip* hydrodynamic boundary conditions.

	δ_ϵ	β_ϵ	Z_{IB}		
	dm ³ mol ⁻¹	dm ⁶ mol ⁻²	$\xi = 0$	<i>stick</i>	<i>slip</i>
FA	29 ± 2	5 ± 2	5.7 ± 0.5	3.6 ± 0.5	4.3 ± 0.5
NMF	155 ± 3	60 ± 3	13.7 ± 0.3	8.9 ± 0.4	10.5 ± 0.4
DMF	17.7 ± 0.6	4.8 ± 0.7	5.9 ± 0.2	3.6 ± 0.2	4.4 ± 0.2

acetonitrile and propylene carbonate [23], solvents with interactions also dominated by dipolar forces. Interestingly the behaviour of FA is very similar to DMF. Here the lack of appropriate data prevents a comparison with solvents of related H-bond structure, like water or diols.

It is commonly assumed that the experimentally accessible dielectric decrement, $\delta_\epsilon = \delta_\epsilon^{eq} + \delta_{KD}$ is the sum of an equilibrium contribution, δ_ϵ^{eq} , comprising irrotational bonding of a number of Z_{IB} solvent molecules in the field of the ions and volume effects, and of a dynamic contribution arising from kinetic depolarization, δ_{KD} [12]. Taking the initial slope a_1 of the solution density in the molarity scale, and M_s and M_{EI} as the molar masses of solvent and electrolyte to express the volume effect yields

$$Z_{IB} = \delta_\epsilon^{eq} L c_s(0) + \frac{a_1 - M_{EI}}{M_s}, \quad (4)$$

where

$$L = \frac{2\epsilon_s^2(0) + \epsilon_\infty^2(0)}{\epsilon_s(0)[\epsilon_s(0) - \epsilon_\infty(0)][2\epsilon_s(0) + \epsilon_\infty(0)]} \quad (5)$$

is defined by the dielectric properties of the neat solvent (concentration $c_s(0)$). Z_{IB} can be compared with solvation numbers from other methods. However, it must be noted that this effective number of solvent dipoles, fixed per equivalent of electrolyte, is a measure for ion-solvent interactions and hence not necessarily equivalent to the geometry defined coordination numbers of the ions.

The correction for kinetic depolarization, δ_{KD} , available from the initial slope of conductance vs. concentration,

$$\delta_{KD} = \xi \cdot \lim_{c \rightarrow 0} \left(\frac{\partial \kappa}{\partial c} \right)_T \quad (6)$$

with the depolarization factor ξ available from theory is still a matter of discussion. The possible limits are given by Chandra et al. [25] suggesting $\xi = 0$, and by the continuum model of Hubbard et al. [26] yielding

$$\xi = p \cdot \frac{\epsilon_s(0) - \epsilon_\infty(0)}{\epsilon_s(0)} \cdot \frac{\tau_{s1}(0)}{\epsilon_0}. \quad (7)$$

In (7) the parameter p characterizes ion transport under *stick* ($p = 1$) or *slip* ($p = 2/3$) hydrodynamic boundary conditions.

Columns 4–6 of Table 5 summarize the corresponding Z_{IB} numbers obtained from the experimental decrements δ_ϵ . For FA and DMF the results are in the range expected for solvents where anion solvation is weak [27] and cation solvation is restricted to the first solvation shell. The considerably larger values obtained for NMF, which compare with Z_{IB} -data obtained for methanol solutions ($Z_{IB}^{slip} = 7.3$ [23]), show that the influence of Na⁺ on the NMF structure is not restricted to the first solvation shell. Although hydrogen bonding between ClO₄⁻ and the solvent molecules may also contribute to Z_{IB} , the probable reason for the large values is an Na⁺-induced reduction of the average NMF chain length, which is also inferred from $\tau_{s1}(c)$ and the concentration dependence of the s_2 process, see below. Comparison of Z_{IB} with the scarce solvation numbers from the literature is not helpful for a decision on the magnitude of the kinetic depolarization correction δ_{KD} . In his review on solvation in non-aqueous solutions Ohtaki quotes Na⁺ solvation numbers n_+ , determined by transference number measurements, of $n_+ = 4$ for FA, $n_+ = 2.6$ for

NMF, and values of 3.0 and 3.3 for DMF [28]. James et al. [29] deduce n_+ (DMF) = 3.4 from Raman spectra whereas Sacco et al. [30] quote n_+ (DMF) = 6 in an NMR study. For the homologous solvent N,N-dimethylacetamide, n_+ (DMA) = 6 for Li⁺ and n_+ (DMA) = 4 for Na⁺ are deduced from infrared studies [31]. Comparison of these data with the results of Table 5 at least suggests that in DMF, but probably also in FA, Na⁺-solvent interactions are strong, but restricted to the first solvation shell.

3.3. Relaxation Time τ_{s1}

For a dispersion step j , where dielectric relaxation originates from the diffusive reorientation of the molecular dipole moment μ_j , the molecular relaxation time, τ'_j , is related to the bulk viscosity η via the extended Stokes-Einstein-Debye equation

$$\tau'_j = \frac{3 V_r}{k_B T} \eta, \quad (8)$$

where the effective volume of rotation, $V_r = V_m f_\perp C$, is determined by the molecular volume of the rotor, V_m , its deviation from spherical shape taken into account by f_\perp , and by the parameter C ($C=1$ for *stick* boundary conditions) coupling the frictional force felt by the rotating particle to η [32]. τ'_j can be estimated from the experimental relaxation time τ_j as

$$\tau'_j = \frac{2\varepsilon_j + \varepsilon_{j\infty}}{3\varepsilon_j} \tau_j. \quad (9)$$

Figure 3 shows the relative change of relaxation time, $\Delta\tau_{s1}(c)/\tau_{s1}(0) = [\tau_{s1}(c) - \tau_{s1}(0)]/\tau_{s1}(0)$, of the s1-process as a function of c/c_s . Having in mind that η increases with electrolyte concentration for all three solvents, cf. Table 1, it is obvious for NMF (curve 2) that the dominating dispersion step does not originate from the rotational diffusion of single molecules. Indeed, the concentration dependence of τ_{s1} resembles that of methanol in NaClO₄ solutions [23]. For the alcohol it was argued that the slow relaxation process probes the probability that different hydrogen-bonded chains “react”, thus lead to a large change of the overall dipole moment [33]. Thus, the increase of the relaxation rate τ_{s1}^{-1} with electrolyte concentration suggests that beyond ion solvation NaClO₄ increases the number of NMF chains by reducing their average length in accordance with the interpretation of $\varepsilon_s(c)$.

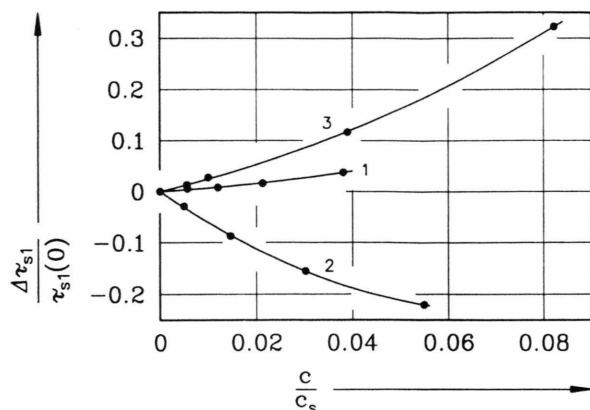


Fig. 3. Relative change $\Delta\tau_{s1}/\tau_{s1}(0)$ of the solvent relaxation time $\tau_{s1}(c)$ as a function of the molar ratio c/c_s of NaClO₄ to solvent in the solution at 25°C for 1: FA, 2: NMF, and 3: DMF.

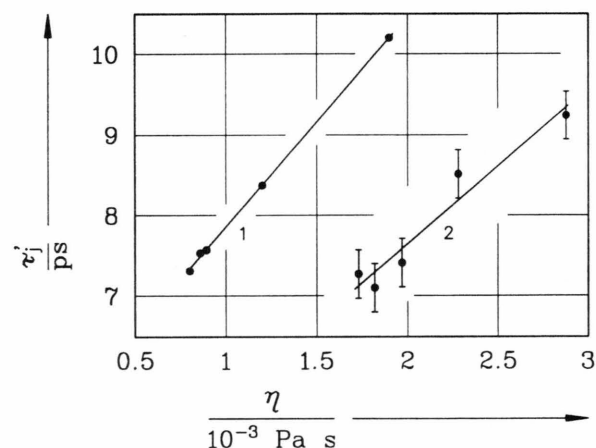


Fig. 4. Molecular relaxation time, τ'_j , of the s1 relaxation process of 1: DMF and of the s2 process of 2: NMF as a function of solution viscosity η at 25°C.

For DMF τ'_{s1} increases linearly with viscosity, see curve 1 of Fig. 4, indicating diffusive reorientation of the solvent dipoles. The slope of $\tau'_{s1} = f(\eta)$, (8), yields as the experimental volume of rotation $V_r^{sl} = (3.57 \pm 0.05) \cdot 10^{-30} \text{ m}^3$, a much smaller value than the molecular volume of $V_m(\text{DMF}) = 144 \cdot 10^{-30} \text{ m}^3$ estimated from intramolecular distances [9] and van der Waals radii [35], whereas $V_r(0) = 12.5 \cdot 10^{-30} \text{ m}^3$ is obtained when the data of neat DMF ($c = 0$) are inserted into (8). A separation of f_\perp and C is not straightforward since DMF is neither a spheroid nor is the dipole vector coinciding with one

of axes of inertia. However, the ratio $V_r(0)/V_m \approx 0.09$ suggests that the rotational motion of the solvent molecules is only weakly coupled to shear stress. Moreover, from $V_r^{sl}/V_r(0) \approx 0.29$ it can be deduced that the electrolyte which creates a marked viscosity increase has only a limited influence on the reorientation of the solvent molecules in the bulk. Hence solution properties seem to be dominated by the large particles formed of Na⁺-ions surrounded by one solvation shell which are immersed in the only weakly perturbed solvent, a behaviour also observed for solutions in acetonitrile [34].

Formamide, $V_m = 50 \cdot 10^{-30} \text{ m}^3$ according to the data of [35, 36], also exhibits an increase of τ_{s1} with increasing c/c_s , see curve 1 of Figure 3. Compared to DMF the values of τ_{s1} and η are roughly increased by a factor of 3 due to the H-bonding network which determines the liquid structure [7]. If (8) is tentatively applied – bearing in mind that the classical definition of rotational diffusion does not apply – the data at $c = 0$ yield $V_r(0) = 10.7 \cdot 10^{-30} \text{ m}^3$ and hence $V_r(0)/V_m \approx 0.21$, reflecting the stronger coupling of dipole reorientation to the environment through hydrogen bonding. However, the influence of ion-solvent interactions on τ_{s1} , expressed by $V_r^{sl} = (0.55 \pm 0.03) \cdot 10^{-30} \text{ m}^3$ and $V_r^{sl}/V_r(0) \approx 0.05$, is very weak. This is also reflected by the only small increase of the relaxation-time distribution parameter α_{s1} . Probably τ_{s1} primarily reflects the formation kinetics of mobile, i.e. non- or single-hydrogen bonded FA molecules from the network in a way similar to aqueous solutions [37], a process only weakly disturbed by the electrolyte in the studied concentration range $c:c_s < 4:100$.

3.4. The s_2 Process of NMF

Comparable to methanol [33], NMF exhibits a small amplitude process (only 0.8% of the total dispersion $\varepsilon - \varepsilon_\infty$ at $c = 0$) with a relaxation time $\tau_{s2} \approx 8 \text{ ps}$, a value in the range expected for the reorientation of a single molecule. Hence an interpretation of the s_2 process in terms of the reorientation of “mobile” NMF molecules seems appropriate. Indeed a plot of τ_{s2}' vs. viscosity, curve 2 of Fig. 4, is linear, and its slope yields an experimental volume of rotation, $V_r^{sl} = (2.7 \pm 0.4) \cdot 10^{-30} \text{ m}^3$. From the data of [8, 35] a molecular volume of $V_m = 80 \cdot 10^{-30} \text{ m}^3$ can be estimated, whereas the data of neat NMF inserted into (8) yield $V_r(0) = 10.7 \cdot 10^{-30} \text{ m}^3$, hence $V_r(0)/V_m \approx 0.07$

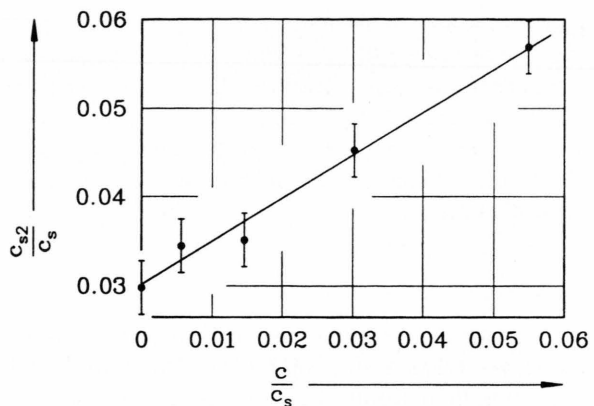


Fig. 5. Relative concentration c_{s2}/c_s of “mobile” NMF molecules as a function of the molar ratio c/c_s of NaClO₄ to solvent in the solution.

and $V_r^{sl}/V_r(0) \approx 0.47$ are obtained. Both ratios are comparable to those of DMF and hence suggest that the – more or less diffusive – reorientation of single molecules is probed. As for methanol, this probably incorporates monomers together with NMF molecules at chain ends involved in a single hydrogen bond.

For process j of a multistep relaxation the concentration c_j of the relaxing species can be inferred from the dispersion amplitude $\Delta_j = \varepsilon_j - \varepsilon_{j\infty}$ and its dipole moment μ_j with the help of Cavell's equation [38]

$$c_j = \frac{2\varepsilon + 1}{3\varepsilon} \cdot \frac{3k_B T \varepsilon_0}{N_A} \cdot \frac{(1 - f_j \alpha_j)^2}{\mu_j^2} \cdot \Delta_j. \quad (10)$$

In (10) α_j is the polarizability of the dipole, and the reaction field factor f_j is accessible from the expressions of Scholte [39].

Taking $\mu_{s2} = \mu(\text{NMF}) = 12.7 \cdot 10^{-30} \text{ C m}$ and $\alpha(\text{NMF}) = 7.69 \cdot 10^{-40} \text{ C}^2 \text{ m}^2 \text{ J}^{-1}$ [40] the relative concentrations c_{s2}/c_s of Fig. 5 are obtained for the data $\Delta_{s2} = \varepsilon_{s2} - \varepsilon_{s3}$ of Table 3. Except for the diffraction study of Neufeind *et al.* [10], who claim that only about 50% of the molecules are hydrogen bonded, to our knowledge no determination of the concentration of monomers and chain ends in liquid NMF is available from the literature. But according to far-infrared spectra, hydrogen bonding seems to predominate even at high dilution in tetrachloromethane [21], and similar values for the monomer fraction are obtained for methanol from various simulation studies, see [33] for references. Therefore, a 3% fraction of mobile NMF molecules in the neat liquid seems plausible. If we assume that the s_2 process is mainly due to the

reorientation of molecules at chain ends the linear increase of slope 0.48 ± 0.04 exhibited by c_{s2}/c_s vs. relative electrolyte concentration, c/c_s , suggests a solute induced increase of the number of hydrogen-bonded NMF chains at the cost of a reduced average length. Hence the conclusions obtained from $\varepsilon_s(c)$ and $\tau_{s1}(c)$ are corroborated.

3.5. The High-frequency Process

All formamides exhibit a fast relaxation process, s2 for FA and DMF, s3 for NMF, of small amplitude and relaxation time around 1 ps – just like water and the lower alcohols [23], see Tables 2–4. Originally it was assumed that this process might monitor the kinetics of H-bond formation for the amphiprotic hydroxylic (water, alcohols) and protophilic H-bond donor (FA, NMF) solvents. However, neither the results from a dielectric study of methanol-tetrachloromethane mixtures [33], nor from an investigation of aqueous electrolytes [37] support the assumption that the high frequency process is a direct measure of the hydrogen-bond life time. For the aprotic protophilic solvents DMF and N,N-dimethylacetamide the hindered intramolecular rotation of the dimethylamino group around the C–N bond is also not a convincing reason for the high frequency mode because of its high activation energy, $\Delta G^* = 87.5 \text{ kJ mol}^{-1}$ [41], in contrast to earlier discussions [16].

FA, NMF, and DMF are asymmetric rotors with the dipole vector not coinciding with an axis of inertia, Fig. 6, so that three relaxation times should be expected. A direct scaling of these τ -values with the moments of inertia, I_j , cannot be expected since hydrodynamic interactions following (8) as well as specific

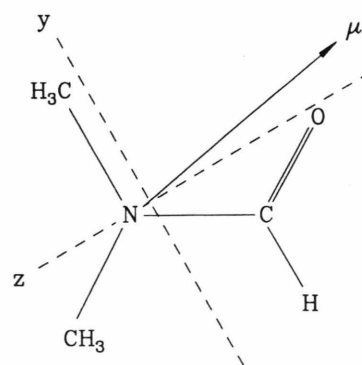


Fig. 6. Dipole vector and axes of inertia of DMF according to [43]. The x-axis is normal to the drawing plane.

	I_x	I_y	I_z
	10^{-47} kg m^2		
FA *	85	74	12
NMF #	148	116	32
DMF *	283	200	94

* Ref. [42], # ref. [21].

Table 6. Moments of inertia I_j of the formamides.

interactions through hydrogen bonding predominate. However, it is obvious from Table 6 that for all formamides I_z is considerably smaller than the other moments of inertia, making rotation around the z-axis the possible origin for the fast relaxation process. This is supported by the isotope effect on the two relaxation times of the polarizability tensor observed by Chang and Castner in their OHD-RIKES study of FA, DMF, and their deuterated homologues [42].

Further support comes from ¹³C NMR relaxation. With this technique Konrat and Sterk [43] recently determined the individual diffusion constants for reorientation of DMF around the axes of inertia and obtained for rotation around the z- and y-axis the correlation times $\tau_z \approx 1.3 \text{ ps}$ and $\tau_y \approx 12.6 \text{ ps}$, which are comparable to $\tau_{s2} = 0.74 \text{ ps}$ and $\tau_{s1} = 10.36 \text{ ps}$, respectively. The small component of μ normal to z might account for the small amplitude $\varepsilon_{s2} - \varepsilon_\infty$.

In [43] also the rotation of the DMF molecule around the x-axis normal to the molecular plane is observed, $\tau_x \approx 85 \text{ ps}$. Such a process is not seen in the complex permittivity spectrum of DMF in spite of the large component of μ and a ratio I_x/I_y which should be sufficient to distinguish the corresponding relaxation times. Possibly this arises from the stacked parallel plate arrangement with antiparallel dipole moments deduced by Yashonat and Rao from their molecular dynamics investigation [44].

For FA and NMF I_x/I_y is closer to unity and hydrogen bonding complicates the relaxation behaviour. Therefore, a possible splitting of the s1 process of FA and of the s2 process of NMF cannot be resolved.

3.6. Ion-pair Relaxation in DMF

In addition to the solvent relaxation processes s1 and s2, the electrolyte solutions of DMF exhibit an additional low-frequency relaxation process centered around 1.5 GHz which is typical for the relaxation of dipolar ion pairs formed by the electrolyte [12]. It is

possible to determine the concentration of ion pairs, c_{IP} , with the help of (10) from the experimental dispersion amplitude $\Delta_{\text{IP}} = \varepsilon - \varepsilon_s$. The ion-pair dipole moment, μ_{IP} , can be calculated as a function of charge separation $d = r_+ + r_- + 2kr_s$ [37]. From c_{IP} the association constants K_A of the model ion-pairs for contact (CIP, $k = 0$), solvent-shared (SSIP, $k = 1$), and solvent-separated (2SIP, $k = 2$) species can be estimated with the extrapolation

$$K_A = \lim_{c \rightarrow 0} \frac{c_{\text{IP}}}{(c - c_{\text{IP}})^2} \quad (11)$$

Taking the ionic radii $r_+ = 98$ pm, $r_- = 240$ pm, and polarizabilities $\alpha_+ = 0.20 \cdot 10^{-40} \text{ C}^2 \text{ m}^2 \text{ J}^{-1}$, $\alpha_- = 5.59 \cdot 10^{-40} \text{ C}^2 \text{ m}^2 \text{ J}^{-1}$ of Na^+ and ClO_4^- , respectively, [45] and the solvent data $r_s = 330$ pm [46] and $\alpha_s = 8.77 \cdot 10^{-40} \text{ C}^2 \text{ m}^2 \text{ J}^{-1}$ [47] the results of Table 7 are obtained. Comparison of the K_A -values with the conductimetrically determined $K_A = 3.2 \text{ dm}^3 \text{ mol}^{-1}$ [46] reveals the solvent-shared ion pair, $k = 1$, as the relaxing species.

This observation is corroborated by the molecular relaxation time of the ion pair, τ'_{IP} , determined from the experimental τ_{IP} -data with the help of the expression

$$\tau_{\text{IP}}^{-1} = (\tau'_{\text{IP}})^{-1} + k_{21} + 2k_{12}(c - c_{\text{IP}}), \quad (12)$$

where k_{12} and $k_{21} = k_{12}/K_A$ are the rate constants of ion-pair formation and decomposition [48]. From the intercept of (12) the value of $\tau'_{\text{IP}} = 260 \pm 30$ ps is obtained, which is between the results of (8) calculated for the geometric parameters of SSIP under the assumption of *stick*, $\tau'_{\text{IP}}(\text{stick}) = 420$ ps, and *slip*

Table 7. Dipole moments of the model ion pairs CIP, SSIP, and 2SIP, and association constants K_A from dispersion amplitudes (this work) and from conductance data, [46].

	k	μ_{IP}	$K_A/\text{dm}^3 \text{ mol}^{-1}$	
		10^{-30} C m	this work	[46]
CIP	0	46.7	70 ± 2	
SSIP	1	159	1.9 ± 1.3	3.2 ± 0.7
2SIP	2	265	0.6 ± 1.3	

boundary conditions, $\tau'_{\text{IP}} = (\text{slip}) = 150$ ps. For the CIP and 2SIP models (8) yields unrealistic results.

The rate constants of ion-pair formation, $k_{12} = (4.7 \pm 0.2) \cdot 10^9 \text{ dm}^3 \text{ mol}^{-1} \text{ s}^{-1}$, and decay, $k_{21} = (1.5 \pm 0.2) \cdot 10^9 \text{ s}^{-1}$ (corresponding to an ion-pair life time of $\ln 2/k_{21} = 460$ ps), are in the range expected for diffusion controlled reactions [49]. Therefore, unlike to other systems, cf. [34, 48], desolvation is not an important step in ion-pair formation.

The synopsis of these results with the information from the solvent relaxation processes suggests that the solution properties of NaClO₄/DMF are dominated by Na^+ -ions with strong ion-solvent interactions restricted to the first solvation shell. These form short-lived complexes on encounter with the essentially unsolvated ClO_4^- -anions but only weakly affect structure and dynamics of the bulk solvent.

Acknowledgements

We are grateful to the Deutsche Forschungsgemeinschaft for generously supporting development of the equipment and experimental work and to the Studienstiftung des Deutschen Volkes for a grant to K.B.

- [1] D. S. Reid and C. A. Vincent, *J. Electroanal. Chem. Interfacial Electrochem.* **18**, 427 (1968).
- [2] J. C. Vaughn, in: J. J. Lagowski (ed.), *The Chemistry of Nonaqueous Solvents*, Vol. II, Ch. 5 Amides, Academic Press, New York 1967.
- [3] K. Weissmehl and H.-J. Arpe, *Industrial Organic Chemistry*, 2nd Ed., VCH, Weinheim 1993.
- [4] Y. Marcus, *Ion Solvation*, Wiley, Chichester 1985.
- [5] J. Barthel and H.-J. Gores, in: G. Mamantov and A. J. Popov (eds.), *Chemistry of Nonaqueous Solutions*, Ch. 1, VCH Publishers, New York 1994.
- [6] H. Ohtaki, A. Funaki, B. M. Rode, and G. J. Reibnegger, *Bull. Chem. Soc. Japan* **56**, 2116 (1983).
- [7] H. Ohtaki and S. Itoh, *Z. Naturforsch.* **40a**, 1351 (1985).
- [8] H. Ohtaki, S. Itoh, and B. M. Rode, *Bull. Chem. Soc. Japan* **59**, 271 (1986).
- [9] T. Radnai, S. Itoh, and H. Ohtaki, *Bull. Chem. Soc. Japan* **61**, 3845 (1988).
- [10] J. Neufeind, P. Chieux, and M. D. Zeidler, *Mol. Phys.* **76**, 143 (1992).
- [11] J. Barthel and R. Buchner, *Pure Appl. Chem.* **63**, 1473 (1991).
- [12] J. Barthel and R. Buchner, *Chem. Soc. Rev.* **21**, 263 (1992).
- [13] J. Barthel, H. Behret, and F. Schmithals, *Ber. Bunsenges. Phys. Chem.* **75**, 305 (1971).
- [14] H. Behret, F. Schmithals, and J. Barthel, *Z. Phys. Chem. NF* **96**, 73 (1975).
- [15] P. Winsor, IV and R. H. Cole, *J. Phys. Chem.* **86**, 2486 (1982).
- [16] J. Barthel, K. Bachhuber, R. Buchner, J. B. Gill, and M. Kleebauer, *Chem. Phys. Lett.* **167**, 62 (1990).
- [17] J. Barthel, R. Wachter, and H.-J. Gores, in: B. E. Conway and J. O'M. Bockris (eds.), *Modern Aspects of Electrochemistry*, Vol. 13, Ch. 1, Plenum, New York 1979.

- [18] J. Barthel, R. Buchner, and H. Steger, *Wiss. Zeitschr. THLM* **31**, 409 (1989).
- [19] J. Barthel, K. Bachhuber, R. Buchner, H. Hetzenauer, and M. Kleebauer, *Ber. Bunsenges. Phys. Chem.* **95**, 853 (1991).
- [20] R. Buchner and J. Yarwood, *Mol. Phys.* **70**, 65 (1990).
- [21] R. Buchner and J. Yarwood, *J. Mol. Liq.* **49**, 141 (1991).
- [22] R. Buchner and J. Yarwood, *Microchim. Acta* **2**, 335 (1988).
- [23] J. Barthel, R. Buchner, K. Bachhuber, H. Hetzenauer, M. Kleebauer, and H. Ortmaier, *Pure Appl. Chem.* **62**, 2287 (1990).
- [24] J. Barthel *et al.*, unpublished results.
- [25] A. Chandra, D. Wei, and G. N. Patey, *J. Chem. Phys.* **98**, 4959 (1993).
- [26] J. B. Hubbard, P. Colonomos, and P. G. Wolynes, *J. Chem. Phys.* **71**, 2652 (1979).
- [27] D. W. James and R. E. Mayes, *J. Phys. Chem.* **88**, 637 (1984).
- [28] H. Ohtaki, *Pure Appl. Chem.* **59**, 1143 (1987).
- [29] D. W. James, R. E. Mayes, W. H. Leong, I. McL. Jamie, and G. Zhen, *Faraday Discuss. Chem. Soc.* **85**, 269 (1988).
- [30] A. Sacco, M. C. Piccinni, and M. Holz, *J. Solution Chem.* **21**, 109 (1992).
- [31] J. Barthel and I. Beer, unpublished results.
- [32] J. L. Dote and D. Kivelson, *J. Phys. Chem.* **87**, 3889 (1983).
- [33] R. Buchner and J. Barthel, *J. Mol. Liq.* **52**, 131 (1992).
- [34] J. Barthel, M. Kleebauer, and R. Buchner, *J. Solution Chem.* **24**, 1 (1995).
- [35] R. C. Weast (ed.), *CRC Handbook of Chemistry and Physics*, 63rd ed., CRC Press, Boca Raton (1982).
- [36] E. Kálmán, I. Serke, G. Pálinkás, M. D. Zeidler, F. J. Wiesmann, H. Bertagnolli, and P. Chieux, *Z. Naturforsch.* **38a**, 231 (1983).
- [37] J. Barthel, H. Hetzenauer, and R. Buchner, *Ber. Bunsenges. Phys. Chem.* **96**, 988 (1992); *ibid.* **96**, 1424 (1992).
- [38] E. A. S. Cavell, P. C. Knight, and M. A. Sheikh, *J. Chem. Soc. Faraday Trans.* **67**, 2225 (1971).
- [39] T. G. Scholte, *Physica* **15**, 437 (1949).
- [40] R. M. Meighan and R. H. Cole, *J. Phys. Chem.* **68**, 503 (1964).
- [41] T. Drakenberg, K.-J. Dahlqvist, and S. Forsén, *J. Phys. Chem.* **76**, 2178 (1972).
- [42] Y. J. Chang and E. W. Castner, Jr., *J. Phys. Chem.* **98**, 9712 (1994).
- [43] R. Konrat and H. Sterk, *J. Phys. Chem.* **94**, 1291 (1990).
- [44] S. Yashonath and C. N. R. Rao, *Chem. Phys.* **155**, 351 (1991).
- [45] J. Barthel, H.-J. Gores, G. Schmeer, and R. Wachter, *Top. Curr. Chem.* **111**, 33 (1983).
- [46] B. S. Krumgalz and J. Barthel, *Z. Phys. Chem. NF* **142**, 167 (1983).
- [47] J. I. Kim, *Z. Phys. Chem. NF* **113**, 129 (1978).
- [48] R. Buchner and J. Barthel, *J. Mol. Liq.*, in press.
- [49] H. Strehlow, *Rapid Reactions in Solution*, VCH, Weinheim 1992.